LAUTECH Journal of Engineering and Technology 8(2)2014: 94 - 99

NUMERICAL INVESTIGATION OF RESTART PROCESS ON HIGH VISCOSITY OIL TRANSPORT IN PIPE

Solomon Oluyemi Alagbe

Department of Chemical Engineering, Faculty of Engineering and Technology, Ladoke Akintola University of Technology, P.M.B.4000, Ogbomoso –Nigeria
Email: alagbeuk@yahoo.co.uk; soalagbe@lautech.edu.ng

ABSTRACT
Numerical investigation of shut in and restart of high viscosity oil-water flow in 1-in ID horizontal pipe was conducted to understand the physical process of restart of high viscous oil that was transported by water assist-annular flow. The knowledge of the restart surges helps in the pump specification and selection. The density and viscosity of oil are 916.2 kgm^{-3} and 3300 and 10000 cP at 25^{o}C. The surges obtained in regaining water assist-annular flows were higher than that of the respective single phase flows. The surge increases with decrease in oil viscosity.

Keywords: Restart, start-up, shut in, shut down, light oil, heavy oil, water assist annular flow

Introduction

The production systems could be shut down during oil production for various reasons, most especially for facility maintenance and work over (Han, 2012).The restart could be a problem due to resistance to flow that is inherent in high viscosity oils. Williams *et al*. (1996) reported that the pressure required to restart flow may exceed the pressure rating of the pump or the pipeline, hence accurate measurements of the Break Away Yield Stress (BAYS) of many waxy crude oils are needed for making informed decisions that can be used during system design.

Transient issues such as restart has become increasingly critical due to movement of oil field developments in deep waters where restoring a shut down system may become difficult after maintenance. How the flow lines and other subsea equipment are treated during a shut down and restart are serious factors during oil production

The restart philosophy has a significant impact on the maximum tieback length, the insulation type chosen, chemical injection line sizes in the umbilical, and the overall chemical storage topside (Golczynski and Nielsen, 2002). Among many typical problems in the oil and gas industry that had been systematically tackled in the production of light oil are poor performance of well in-flow, excessive pumping power requirements, low efficiency of Electric Submersible Pumps (ESP's), topsides problems associated with water separation due to emulsions and degassing of the oil and restart problems that often follow the pressure build-up in the flow lines (Mehta *et al*, 2004). However, one of the challenges facing the engineers in the oil production is the question of how to design pipeline and subsea systems for an economical and safe transport of the multiphase fluids from the well bottom to the processing plant (Lin *et al.,* 2005). This challenge brought about flow assurance for identifying, quantifying and mitigating all flow risks that are associated with oil production.

There are three possibilities for the start of flow when a constant pressure is applied to the pipeline depending on the wall shear stress; the possible restarts are start-up without delay, start-up with delay and unsuccessful start-up (Chang,1999). Start-up without delay is a situation where the applied pressure results in the wall shear stress that is higher than the static yield stress of the oil. In this case, the flow starts immediately, but when the wall shear stress lies between the static yield stress and the elastic limit yield stress at the start point, the start-up experiences a delay. In start-up with delay, the flow will start after a delay time since no oil in the pipe yields to the pressure. The last case is the unsuccessful start-up where the wall shear stress is less than the elastic yield stress.

Several studies on restart philosophy in oil production of low viscosity oils with wax content have been reported (Chang *et al*., 1999; Davidson *et al*.,2004 and Vinay *et al*., 2007) in which wax has been identified to play dominant role in the possibility of restarting a shutdown flow operations. This is prevalent especially during

either planned or unplanned shut down maintenance of waxy crude oil production system. Other researchers like Mehta *et al* (2004) and Guevara *et al* (1997) mentioned the need to verify the impact of high viscosity of oil in the restart problems. Mehta *et al* (2004) affirmed that the facts that heavy oils are often characterized by their high viscosity, low API gravity and reservoir energy and tendency to form emulsions, make the production and transportation of heavy oils a major challenge from a flow assurance perspective. Guevara *et al.* (1997) in comparing different transportation methods for heavy oil, highlighted that restart could be problematic when adopting some methods like heating, annular core flow and emulsion means of producing oil through flow lines. However there is paucity of information on the restart behaviour of high viscosity oil -water flow. Bensakhria *et al* (2004) suggested that restart need to be studied in order to guaranty the complete feasibility of the core annular flow for an industrial scale.

In a typical restart study, varying pressure is always employed to determine the pressure at which the waxy crude oil gels will yield due to its viscoplastic behaviour, but in the current study, the injection of water for the transportation of heavy oil is the major factor for examining the restart process. The oils used have been de-waxed but possess high viscosity, and hence the behaviour might not be comparable to waxy crude but viscous enough to represent heavy oils. The choice of the Water Assist-Annular (WA-ANN) flow is crucial because it is the regime that is cost effective for the transport of high viscosity oil. This study is necessary to resolve the application of full navier-stokes to address restart of high viscosity oil based water assist-annular flow in horizontal pipe.

Model and Simulation

The governing equations employed in Computational Fluid Dynamic (CFD) are the mass conservation equation (also known as continuity equation), and Navier-stokes equation (also known as momentum equation).

Model Assumptions

Some of the assumptions considered in setting up this model are outlined below.

- **i.** The flow is not axisymmetrical.
- **ii.** The liquid phases are incompressible.
- iii. The pressure in the radial direction is constant.
- iv. The diameter of the pipe is sufficiently small compare with its length; the pipe is long enough for the flow to develop.
- v. The effect of temperature is negligible

Model Equations

The equation for conservation of mass (or continuity equation) and momentum are given Ansys Inc., (2003) and Bird *et al*., (2006) as equations (1) and (2), respectively

$$\frac{\partial}{\partial t}(\rho) + \nabla \cdot (\rho \vec{v}) = 0 \quad (1)$$

A momentum equation is used for the Viscous Oil Flow (VOF). This depends on the volume fractions of all phases in the flow through density and viscosity parameters as follows:

$$\frac{\partial}{\partial t}(\rho \vec{v}) + \nabla \cdot (\rho \vec{v}\vec{v}) = -\nabla P + \nabla \cdot \left[\mu\left(\nabla \vec{v} + \nabla \vec{v}^{T}\right)\right] + \rho \vec{g} + \vec{F} \quad (2)$$

Where $\vec{F}$ is a body force, and μ is the viscosity of the phase. The tracking of the interface(s) between the phases is accomplished by the solution of a continuity equation for the volume fraction (α) of one (or more) of the phases. For the qth phase, equation (2) has the form of equation (3):

$$\frac{\partial \alpha_q}{\partial t} + \nabla \cdot (\alpha_q \vec{v}) = \frac{S\alpha_q}{\rho_q} \quad (3)$$

Where S is a source. The primary-phase volume fraction will be computed based on the constraint in equation (4):

$$\sum_{q=1}^{n} \alpha_q = 1 \quad (4)$$

The geometric reconstruction scheme was used to calculate the fluxes at control volume faces required by the VOF model.

Turbulence models

Standard k-epsilon model

In order to simulate turbulence in this work, one of the popular RANS turbulent models, low-Reynolds-k-epsilon was used. The reason for this model is that it has demonstrated capability to properly simulate many industrial processes including multiphase flow. The model is described by the equations (5) - (8):

$$\frac{\partial}{\partial t}(\rho k) + \frac{\partial}{\partial x_j}(\rho k u_j) = \frac{\partial}{\partial x_j}\left[\left(\mu + \frac{\mu_t}{\sigma_k}\right)\frac{\partial k}{\partial x_j}\right] + P_k + P_b + \rho\varepsilon - Y_M + S_k \quad (5)$$

$$\frac{\partial}{\partial t}(\rho \varepsilon) + \frac{\partial}{\partial x_j}(\rho \varepsilon u_j) - \frac{\partial}{\partial x_j}\left[\left(\mu + \frac{\mu_t}{\sigma_\varepsilon}\right)\frac{\partial \varepsilon}{\partial x_j}\right] \quad (6)$$

Where

$$\mu_t = \rho C_\mu \frac{k^2}{\varepsilon} \quad (7)$$

$$C_{1\varepsilon} = 1.44, \qquad C_2 = 1.9, \qquad \sigma_k = 1.0, \quad (8)$$

Geometry, mesh and boundary conditions

In order to investigate the flow behavioural details observed in the experimental high viscosity oil-water flow rig, a 1-in horizontal pipe geometry was employed. It is 3-Dimensional and its longitudinal cross section is illustrated in Figure 1. It is a 5m long, 1-in internal diameter horizontal pipe similar to the experimental arrangements. The pipe axis is aligned with the z-axis and several measurements sections are placed along the pipe.

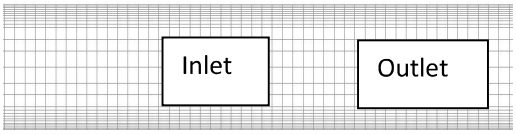

Figure 1: Longitudinal Cross Section of the Mesh

The geometry and mesh that were used in this study were developed with Gambit 2.4 and imported into FLUENT 12.1 for the case simulations. The concentric inlet design was only considered in the CFD simulation to impose the water injection as shown in

Figure 2 where water was injected in the annulus and oil injected at the centre.

Figure 2: CFD Annular Flow Inlet Geometry Description

The region near the wall was meshed finer than the rest of the cross section, as it contains greater amount of gradients. A mesh sensitivity analysis was conducted to identify the minimum mesh density that ensures that the solution is independent of the mesh size. The outcome over 30 seconds flow time is presented in Figure 3. The Eulerian-VOF CFD model was used to study the flow of oil-water. The improvement introduced as User Defined Function (UDF) into the oil-water turbulence Launder Sharma Low Reynolds k-epsilon (LRKE) model was also employed. The CFD results were validated using measurements of pressure gradient obtained from the experiments. Constant superficial velocities and atmospheric pressure were specified at the inlet and pressure outlet at the outlet boundaries of the CFD models. The temperature change along the channel was considered negligible. The relevant properties of the two fluids (oil and water) used in the simulation are as given in Table 1. The pre-validation tests were conducted using pressure drop data from experiment setup and empirical correlation of a single liquid phase of water and oil (Figure 4a and 4b).

Table 1: Fluid Properties

Fluid	Density @25°C (kg/m^3)	Viscosity @25°C (Pa.s)	Surface Tension @19°C (N/m)
Water	998.2	0.001003	
Oil	916.2	3.3, 10.0	0.026

Boundary Conditions

Appropriate and commonly encountered boundary conditions at the boundaries for computing the flow in a particular computational domain are employed in this research and stated below:

Inlet: Provide distributions of k *and* ε along with flow properties, i.e., velocity and temperature, in the corresponding real situation. In some cases, it is difficult to obtain values of k *and* ε at the inlet and in such cases these can be obtained based on an approximation from the turbulent intensity Ti and a characteristic length L of the flow configuration:

$$l = 0.07L$$

where l denotes a turbulent length scale and L characteristic length.

Outlet: At the outlet usually turbulence k *and* ε is taken equal to zero, the mean temperature (T_m) equal to the ambient temperature (T_1) and pressure (p) equal to the atmospheric pressure (p_1).

Wall: At the solid wall either the no slip condition using the low-Re version was applied.

Solution Method

Finite Volume Method (FVM) discretisation scheme in Fluent 12.1 with an algebraic segregated solver and co-located grid arrangement was implemented to solve the system of partial and ordinary differential equations. In this grid arrangement pressure and velocity are both stored at cell centres. Versteeg and Malalasekera, (2007) explain the details of the FVM discretisation. Since FLUENT uses a segregated solver, the continuity and momentum equations need to be linked, hence PISO algorithm which stands for Pressure Implicit with Splitting of Operators by Issa, (1986) was employed because of its good performance to find a fast converged solution. PISO is a pressure-velocity calculation procedure that involves one predictor step and two corrector steps.

Flow regimes are known to be periodical in nature hence the unsteady solver was employed to simulate the flow behaviours. Since statistically steady-state of the flow behaviours are made up of several periodic flows the time employed to collect data in the experiments was adopted i.e. 30s. The variable time step method was adopted to prevent divergence and also to reduce the computation time of CPU. The time step was adjusted automatically based on the Courant numbe known as CFL after its authors (Courant-Friedrich-Lewy). The Courant number is a dimensionless number that compares the time step (Δt) in a calculation to the characteristic time of transit for a fluid element across a control volume. The global CFL condition is given by

$$CFL_{global} = \Delta t_{global} * max\left(\sum \frac{outgoing\ fluxes}{volume}\right) \quad (10)$$

where Δt_{global} is the global time step. The global Courant number employed in this research was 2 and the resulting time step varied from $1e^{-05}$ to 0.004s. Here a static contact angle (θ=90°) is applied for all simulation cases. The simulation for each flow condition was run from time t=0s until the flow developed and stabilised for about 15s before the flow was shut down for 5s by switching both oil and water velocities to zero. The restart condition kicked off at the end of 5s shut down (i.e. overall 20s) with the former constant oil and water flow superficial velocities and ran for another 10s.

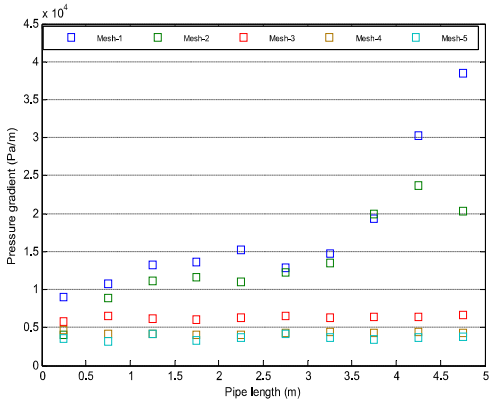

Figure 3: Pressure Gradients of the Mesh Profiles

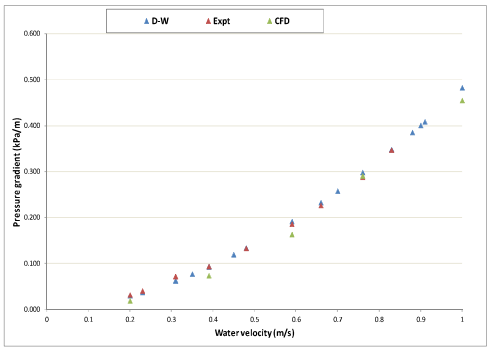

Figure 4a: Comparison Of D-W, Experimental and CFD Pressure Gradients of a Single Phase Water in 1-In ID 5m Long Pipe

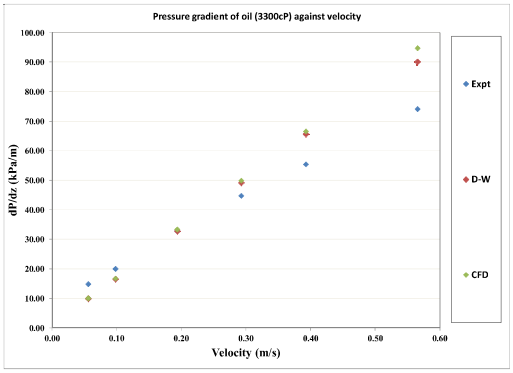

Figure 4b: Comparison of CFD, D-W and Experimental Pressure Gradients of a Single Phase Oil in 1-in ID 5m Long Pipe.

Result and Discussion

The restart trend plots for oil viscosity at 3300 cP is shown in Figure 5 to Figure 7. All the plots reflect similar behaviour. Prior to restart at 20s, the plots reveal relatively zero pressure since there was no flow in the pipe. The spike in the pressure trends in Figure 5 to Figure 7 could be explained as a result of acceleration after a restart which caused additional pressure surge and pressure drop due to the change in the momentum of the fluid. This assertion is in agreement with Tang and Wong (2005) who observed similar trend in their study of flow assurance of crude oil with severe emulsion.

The pressure surge and drop occurred gradually as presented in Figure 5 and Figure 8 showing that there is a delay over a period of time to overcome the spike. These figures further reveal that the magnitudes of the pressure surge is a function of the flow velocities. For oil viscosity at 3300 cP in the presence of water the surge increases with increase in water superficial velocities (Vsw) and the highest surge is recorded when the Vsw is very high (i.e. high water cut). On the other hand, when the oil viscosity was raised to 10000 cP, a reverse of the output of 3300 cP was observed when the

Vsw was increased from 0.21m/s to 0.30m/s; the surge decreases with increase in Vsw (or water cut) but increases again when the Vsw was further increased. This behaviour is not yet understood.

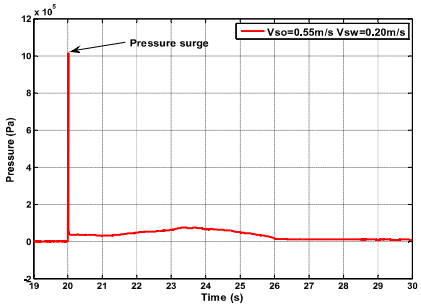

Figure 5: Plot of Restart Process for 3300 cP Oil at 0.55m/s Oil Superficial Velocity and 0.20m/s Water Superficial Velocity

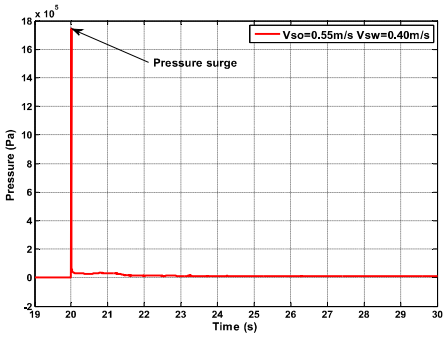

Figure 6: Plot of Restart Process for 3300 cP Oil at 0.55m/s Oil Superficial Velocity and 0.40m/s Water Superficial velocity

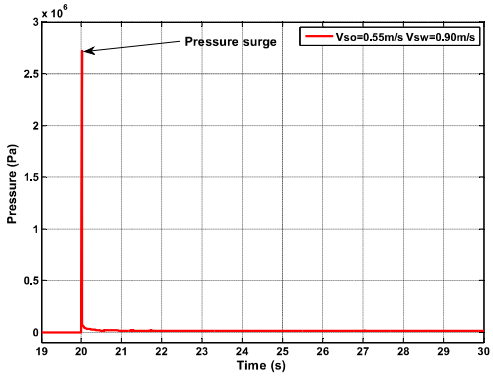

Figure 7: Plot of Restart Process for 3300 cPOil at 0.55m/s Oil Superficial Velocity and 0.90m/s Water Superficial Velocity

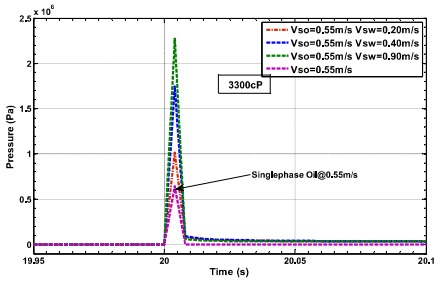

Figure 8: Comparison of Pressure Surges at Different Flow Conditions for 3300 cP Oil

Table 1: Restart Pressure of 3300 cP at Different Velocities

Vso, Vsw (m/s)	Restart Pressure MPa
(0.55, 0.00)	0.647
(0.55, 0.20)	1.014
(0.55, 0.40)	1.744
(0.55, 0.90)	2.723

Comparing the restart output of single phase oil at 3300 cP and 10000 cP from Figure , it could be observed that 3300 cP oil has higher surge than 10000 cP. This could be traced to the viscosity difference which favours 3300 cP oil to gain more acceleration than 10000 cP. In this case, it could be inferred that the higher the viscosity of a fluid the lower the surge tendency provided it flows alone. In addition, when the restart results of single phase oil are compared with that of two phase oil-water flow as shown in Figure 7 and Figure 8, it could be seen that the surges of single phase are an order of magnitude lower than that of two-phase oil-water flows

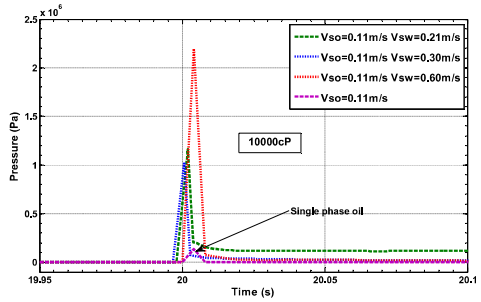

Figure 9: Comparison of Pessure Surges at Different Flow Conditions for 10000 cP oil

Table 2: Restart Pressure of 10000 cP at Different Velocities

Vso, Vsw (m/s)	Restart Pressure MPa
(0.11, 0.00)	0.136
(0.11, 0.21)	3.214
(0.11, 0.30)	1.025
(0.11, 0.60)	2.194

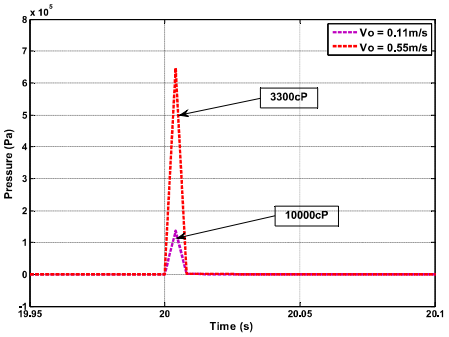

Figure 10: Comparison of Restart Pressure Surges at Different Oil Viscosities

Conclusion

The restart pressure requirement was investigated on the shutdown of water assist annular flow regimes using CFD, considering only the isothermal situation in which both the oil and the displacing/carrier fluid (water) are considered as incompressible fluids.

References

Bensakhria, A., Peysson, Y. and Antonini, G. (2004). Experimental Study of the Pipeline Lubrication for Heavy Oil Transport. *Oil & Gas Science and Technology,* 59(5):523-533.

Chang, C., Nguyen, Q. D. and Rønningsen, H. P. (1999). Isothermal Start-Up Of Pipeline Transporting Waxy Crude Oil. *Journal of Non-Newtonian Fluid Mechanics*, 87(2):127-154.

Davidson, M. R., Dzuy Nguyen, Q., Chang, C. and Rønningsen, H. P. (2004). A Model For Restart of a Pipeline with Compressible Gelled Waxy Crude Oil. *Journal of Non-Newtonian Fluid Mechanics,* 123(2):269-280.

Golczynski, T.S. and Niesen, V.G. (2002). Thermal Behavior during Restart of Ultradeepwater Flowlines. *Proceedings of SPE Annual Technical Conference and Exhibition*, September 29 - October 2, San Antonio, Texas, SPE-77574-MS..

Guevara, E., Gonzalez, J. and Ninez, G. (1997). Highly Viscous Oil Transportation Methods in the Venezuelan Oil Industry. *Proceeding of 15th World Petroleum Congress,* October 12 -17, Beijing, China, WPC-29199.

Han, G., Ling, K., Khor, S., Zhang, H. and Zhang, H. (2012). Simulation of Multiphase Fluid-Hammer Effects During Well Shut-In And Opening. *Proceedings of Asia Pacific Oil and Gas Conference and Exhibition*, October 22-24,Perth, Australia.

Issa, R. (1986). Solution of The Implicitly Discretised Fluid Flow Equations by Operator-Splitting. *Journal of Computational Physics*, 62(1): 40-65.

Lin, T. R., Guo, B., Song, S., Ghalambor, A. and Chacko, J. (2005). *Offshore pipelines,* 1st Edition, Gulf Professional Publishing,.

Mehta, A., Zabaras, G., Schoppa, W. and Peters, D. (2004). Unlocking Deepwater Heavy Oil Reserves-A Flow Assurance Perspective. *Offshore Technology Conference.*

Tang, Y. and Wong, S. (2005). A Flow Assurance Study for a Satellite Crude Oil System With Severe Emulsion. *SPE Annual Technical Conference and Exhibition.*

Versteeg, H. K. and Malalasekera, W. (2007). *An Introduction to Computational Fluid Dynamics: the Finite Volume Method*, Prentice Hall.

Vinay, G., Wachs, A. and Agassant, J. (2006). Numerical Simulation of Weakly Compressible Bingham Flows: The Restart of Pipeline Flows of Waxy Crude Oils. *Journal of Non-Newtonian Fluid Mechanics,* 136(2): 93-105.

Vinay, G., Wachs, A. and Frigaard, I. (2007). Start-Up Transients and Efficient Computation of Isothermal Waxy Crude Oil Flows. *Journal of Non-Newtonian Fluid Mechanics,* 143(2): 141-156.

Williams, T., Hsu, J. and Patterson, H. (1996). Measurement of Break Away Yield Stress of Waxy Crude Oil And Pipeline Restart System Design. *Offshore Technology Conference.*